Performance Evaluation of a Newly Developed Transition Metal-doped HZSM-5 Zeolite Catalyst for Single-step Conversion of C1-C3 Alcohols to Fuel-range Hydrocarbons

Supplementary Information *(SI)*

1. **Catalyst Characterisation**

1.1. Phase Identification

The as-synthesised ZSM-5 displays a similar crystalline phase as the standard ZSM-5 represented by JCPDS reference No. 96-154-0268, as indicated by its XRD pattern. *SI.* Figure 1a shows that the most prominent peaks of the pure and modified HZSM-5 appear at 2θ = 7–9° and 23–24° [1-3]. The distinct diffraction peaks observed at 7.97°, 8.88°, 14.81°, 23.14°, 23.32°, and 24.00° correspond to reflective planes (101), (200), (301), (501), (303), and (131) of the MFI framework of the ZSM-5 catalyst, indicating that introduction transition metals (Ni, Fe and Co) into ZSM-5 did not alter the framework of the material [2]. According to the XRD analysis, the content (0.5 wt%) transition metal species were either too small or amorphous to form XRD signals or incorporated into the zeolite structure, which does not indicate the presence of metal (Ni, Fe, and Co) oxides [4].

1.2. Functional Group Identification – FTIR

The absorption spectra of protonated as-synthesised and metal-doped ZSM-5 are depicted in Figure 1b, within a range of 4000 to 400 cm^{-1}. The absorption peaks of ZSM-5 in *SI.* Figure 1b, located at 440, 543, 792, 1064, 1218, 1633, and 3646 cm^{-1}, are in satisfactory agreement with the ZSM-5 reference data [5, 6] (Table 1). The crystal framework studied by XRD and FTIR shows that the synthetic conditions used to prepare the as-synthesised and metal-doped ZSM-5 were effective, and only the ZSM-5 zeolite phase was detected in agreement with the literature [5, 7, 8]. However, the low concentration of incorporated metal species may not be sufficient to create the characteristic peaks of respective metal oxides, as the FTIR spectra do not show any identifiable bands of these oxides (Ni, Co, and Fe).

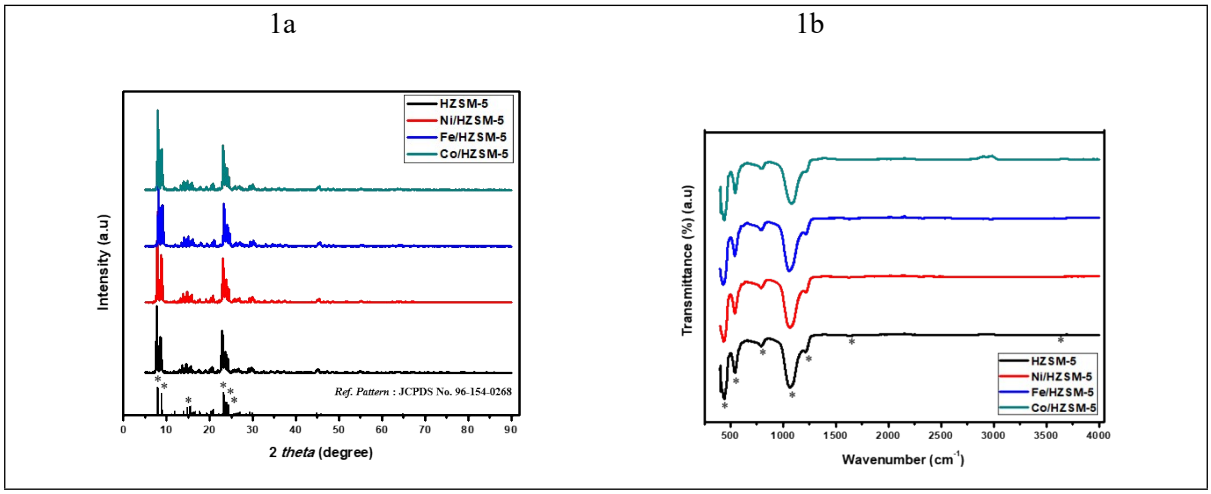

SI. Figure 1 (a) XRD (b) FTIR of unmodified and metal-doped HZSM-5 catalysts

SI. Table 1. FTIR wavenumbers and representations for ZSM-5 catalyst

FTIR wavenumber (cm^{-1})	Representation	Ref.
440	Tetrahedron units of SiO_4 and AlO_4	[8]
543	Pentasil zeolite structure's five-membered ring	[8]
792	Siloxane groups in a symmetrical manner	[5]

1064 and 1218	External and internal asymmetric stretching vibrations of the T-O band	[5]
1633	Deformational vibrations of water molecules	[5]
3646	Siloxane and hydroxyl groups	[7]

1.3. Catalyst Morphology, Particle Size Distribution and Elemental Composition

Micrographs of HZSM-5 and Ni/HZSM-5 zeolites were obtained using high-resolution scanning electron microscopy and are presented in *SI.* Figure 2. The SEM images allow for observing particle sizes, morphology, and aggregation in both as-synthesised and metal-doped HZSM-5 crystals. At high magnification, prismatic crystals and the aggregation of nanosized crystals into microspheres are observed. Smaller particles can be seen on the microspheres due to the high nucleation density and slow crystal development following nucleation. Since the HZSM-5 particles developed into larger aggregates composed of many separate or intergrown zeolite particles, estimating the primary particle size using SEM images alone is challenging. For both as-synthesised and metal-doped HZSM-5, larger crystal aggregate dimensions range from 100 to 1000 nm. PSD analysis results (inset Figures) show that the particle size distribution for HZSM-5 and Co/HZSM-5 is in the range of 0.5-100 um, while Fe/HZSM-5 and Ni/HZSM-5 is between 0.4 um (min) and >100 um (max). The presence of transition metal species results in a bimodal distribution, which can be attributed to various growth processes, particle breakup, and large particles in the system. The larger mode of the distribution results from redispersion or breakup, while the smaller mode represents molecular condensation [9, 10]. The particle average particle sizes for the catalyst are 4.3, 4.5, 5.5, and 5.45 µm for Co/HZSM-5, HZSM-5, Ni/HZSM-5, and Fe/HZSM-5, respectively. Previous research suggests that the presence of highly dispersed particles can be attributed to transition metals (Ni, Fe species, and Co-cations or oxo-cations) initially located in zeolite channels, while the introduction of these metal species is responsible for the formation of large particles. A similar trend has been reported in other studies [11-14]. The transition metals content in the metal-doped zeolites was determined by means of elemental analysis (EDS and XRF), as shown in *SI.* Table 2.

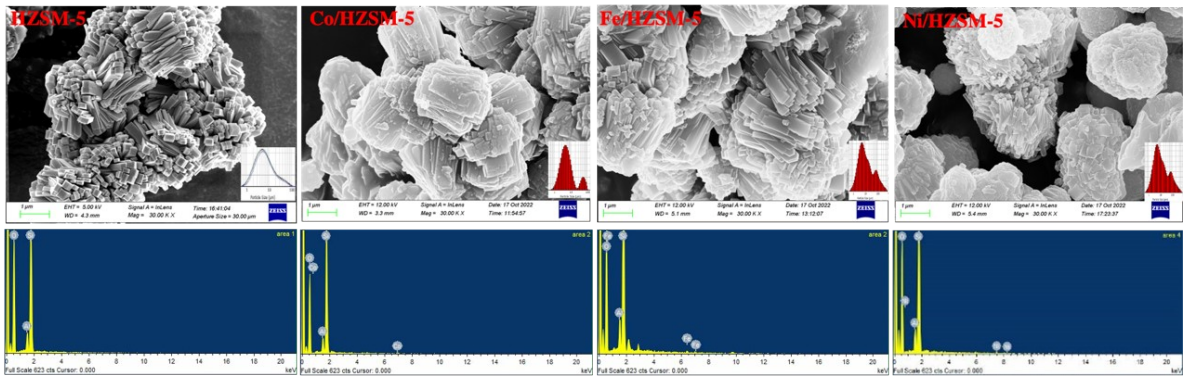

SI. Figure 2. SEM images and corresponding EDS spectra and (inset figures) PSD of modified and metal-doped HZSM-5 catalysts

SI. Table 2. Quantitative analysis of metal-doped samples (EDS & XRF results)

Catalysts	Metal Loading (wt.%)		
	Amount Loaded	EDS Avg.	XRF
HZSM-5	0.0	0.0	0.0
Co/HZSM-5	0.5	0.34	0.48

Fe/HZSM-5	0.5	0.54	0.55
Ni/HZSM-5	0.5	0.71	0.50

1.4. Textural Properties

The low-temperature N_2 adsorption-desorption isotherm of the zeolite catalysts was examined using the BJH method. N_2 adsorption–desorption measurements were employed to determine the BET surface area of Ni/HZSM-5, Fe/HZSM-5, and Co/HZSM-5 catalysts and the HZSM-5 support. The BET surface area of the doped zeolites decreased from 397.5 $m^2\ g^{-1}$ for HZSM-5 to 381.36, 387.20, and 362.60 $m^2\ g^{-1}$ for Ni/HZSM-5, Fe/HZSM-5, and Co/HZSM-5 catalysts, respectively, as shown in *SI.* Table 3. This suggests that the surface of ZSM-5 was covered by metal (Ni, Fe, and Co) species, partially blocking zeolite channels [15, 16]. Additionally, the total pore volume of the catalysts decreased from 0.706 $cm^3\ g^{-1}$ for HZSM-5 to 0.590, 0.448, and 0.461 $cm^3\ g^{-1}$ for Ni/HZSM-5, Fe/HZSM-5, and Co/HZSM-5 catalysts, respectively, while the pore diameter slightly decreased from 2.2 nm for ZSM-5 to 2.02, 2.00, and 2.01 nm for Ni/HZSM-5, Fe/HZSM-5, and Co/HZSM-5, respectively. This provides further evidence that Ni, Fe, and Co species coated the external surface of HZSM-5, significantly clogging zeolite channels and hindering the entry of N_2 into pores [15, 17]. Moreover, as-synthesised and metal-doped catalysts' surface area and pore volume were generally sufficient for effective heterogeneous catalysis. Notably, the decrease in the total pore volume of the metal-doped catalysts was caused mainly by a drop in the macropore volume, as determined by the BJH method [18].

Figure 3a shows the N_2 physisorption isotherms of the as-prepared and metal-doped samples, while *SI.* Figure *(inset)* 3b & c presents the corresponding pore size distribution for adsorption and desorption. All isotherms exhibited a mixture of a type IV isotherm and an H4-type hysteresis loop [18, 19], with the hysteresis loop occurring at a relatively higher pressure than P/P0 > 0.4, indicating the presence of both micropores and mesopores. These hysteresis loops are typically associated with the capillary filling and condensation of N_2 within the uniform slit-shaped intercrystalline mesopores generated by the aggregation of nanosized zeolite crystals [18]. Although the relative pressure had a positive correlation with the amount of absorbed volume, the amount of adsorption decreased as transition metals were introduced, following the order (volume adsorbed at STP) HZSM-5 (109.94) > Fe/HZSM-5 (108.58) > Ni/HZSM-5 (104.61) > Co/HZSM-5 (102.39 $cm^3\ g^{-1}$), which correlated with the decrease in S_{BET} and S_{micro} surface area of the samples.

SI. Table 3. Textural properties of unmodified and metal-modified HZSM-5 catalysts

Catalysts	**S_{BET} ($m^2\ g^{-1}$)**	**S_{micro} ($m^2\ g^{-1}$)**	**$V_{total\ (BJH)}$ ($cm^3\ g^{-1}$)**	**$V_{meso\ (BJH)}$ ($cm^3\ g^{-1}$)**	**$V_{macro\ (BJH)}$ ($cm^3\ g^{-1}$)**	**Avg pore dia. (nm)**	**Volume @STP ($cm^3\ g^{-1}$)**	**Metal loading (wt.%)**
HZSM-5	397.48	335.21	0.7059	0.6775	0.0285	2.22	109.94	0.0
Co/HZSM-5	362.60	312.39	0.4612	0.4555	0.0057	2.01	102.39	0.5
Fe/HZSM-5	387.20	331.35	0.4484	0.4478	0.0006	2.00	108.58	0.5
Ni/HZSM-5	381.36	318.91	0.5903	0.5820	0.0083	2.02	104.61	0.5

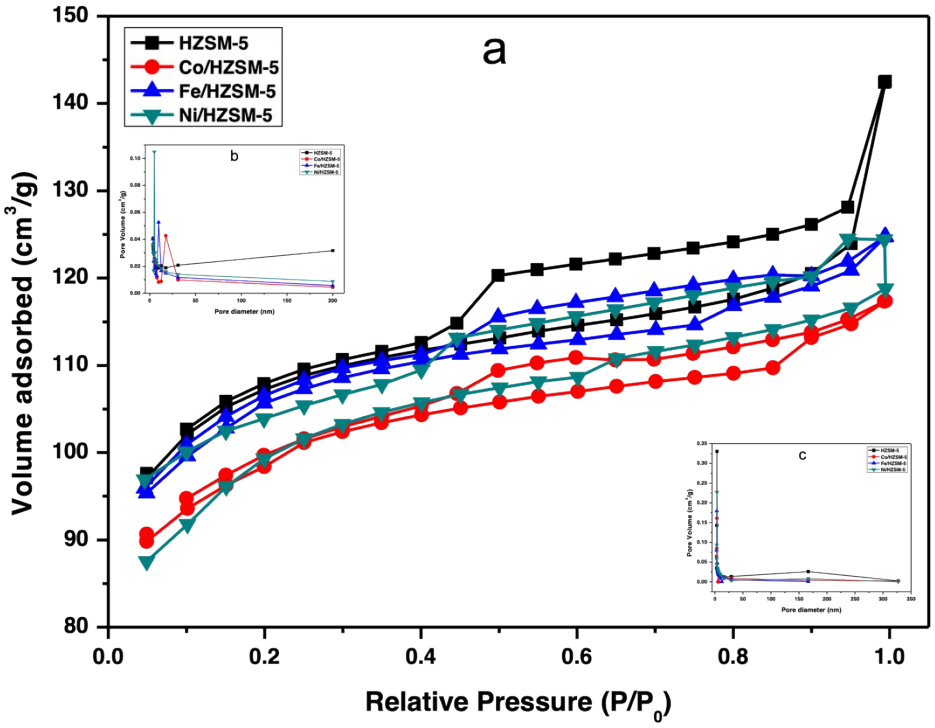

SI. Figure 3 (a) N_2 adsorption-desorption isotherm. *Inset figures* - BJH pore size distribution for (b) adsorption and (c) desportion of pure and transition metal-doped HZSM-5 catalysts

1.5. NH_3-TPD Results

SI. Table 4 presents the findings from ammonia temperature-programmed desorption (TPD) analysis conducted on pure HZSM-5 zeolite and metal-modified HZSM-5 catalysts. The TPD analysis revealed three distinct desorption bands occurring at different temperature ranges: 180-200 °C, 400-450 °C, and 650-700 °C, corresponding to weak, moderate, and strong acid sites, respectively. The desorption band in the 180-200 °C range can be attributed to physically and weakly chemically adsorbed ammonia, while the band in the 400-450 °C range indicates NH_3 adsorbed on the zeolite's hydroxyl groups. The 650-700 °C desorption band is associated with the dehydroxylation and desorption of NH_3 from the zeolite's strong Brønsted or Lewis acid sites [20, 21]. Upon incorporating metal species into HZSM-5, the acid characteristics undergo changes, including an increase in weak acid sites and a decrease in moderate and strong acid sites. These changes in acidity are accompanied by shifts in peak temperatures, which can be attributed to the interaction between the zeolite framework and the metal species. The weak acid sites exhibited increases of 9.52 %, 5.90 %, and 10.41 % at peak temperatures of 189 °C, 194 °C, and 190 °C, respectively, for the Co-, Fe-, and Ni-doped catalysts compared to the unmodified HZSM-5 catalyst with 0.95 mmol/g at 198 °C. Among the metal-doped catalysts, the Ni-doped catalyst showed the highest increase in weak acid sites. The number of moderate acid sites slightly increased by 6.3% at a peak temperature of 436 °C for the Fe-doped catalyst, while Co- and Ni-doped catalysts exhibited decreases of 6.81 % within this temperature range. A significant decrease in strongly acid sites was observed for all metal-doped catalysts, resulting in decreases of 27.52 %, 29.20 %, and 41.71 % compared to the unmodified HZSM-5 catalyst. However, despite the decline in strong acid sites, the

modification of transition metals led to an overall increase in the total acidity of the respective catalysts.

Several studies have shown that adding transition metals (Co, Fe and Ni) can reduce the number of strong acids in the catalyst [15, 21-24]. The reason for this effect is primarily due to the electronic interactions between the metal species and the framework of the ZSM-5 zeolite. The tetrahedral units of Si and Al in the ZSM-5 zeolite are negatively charged and balanced by positively charged cations, such as protons (H^+). The protons attached to the oxygen atoms in the zeolite framework act as strong acid sites responsible for the acidity and catalytic activity of the catalyst. When metal species are doped into the ZSM-5 catalyst, they can replace some protons and occupy the cationic positions within the zeolite framework. The doped species are typically Co^{2+}, Fe^{3+}, and Ni^{2+} ions. These ions have lower positive charge density than protons, resulting in weaker electrostatic interaction with the oxygen atoms of the framework. As a result, the metal-doped ZSM-5 catalyst exhibits reduced strong acidity as the less acidic metal ions replace the strongly acidic sites (protons). The weaker acid sites provided by the metal species result in a decrease in strong acidity with a concomitant increase in weak acid sites [25, 26]. It should be noted, however, that the decrease in strong acid sites is not always desirable because the catalytic performance of ZSM-5 may depend on the presence of these strong acid sites for some catalytic reactions. For the present study, the deliberate incorporation of metal species aims to modify the catalytic behaviour of ZSM-5 and facilitate alternative reactions or selectivities that do not depend solely on strong acid sites.

SI. Table 4. NH_3-TPD of unmodified and metal-modified catalyst

Catalysts	Peak Temp (°C)			Acidity conc. (mmol NH_3/g)			
	L.T.	M.T.	H.T.	Weak	Moderate	Strong	Total acidity
HZSM-5	198	419	686	0.95	0.74	0.024	1.714
Co/HZSM-5	189	425	667	1.05	0.69	0.015	1.755
Fe/HZSM-5	194	436	678	1.01	0.79	0.017	1.817
Ni/HZSM-5	190	435	688	1.06	0.69	0.014	1.764

Reference

[1] G. Reding, T. Mäurer, and B. Kraushaar-Czarnetzki, "Comparing synthesis routes to nano-crystalline zeolite ZSM-5," *Microporous and mesoporous materials,* vol. 57, no. 1, pp. 83-92, 2003.

[2] M. Yang *et al.*, "Conversion of lignin into light olefins and aromatics over Fe/ZSM-5 catalytic fast pyrolysis: Significance of Fe contents and temperature," *Journal of analytical and applied pyrolysis,* vol. 137, pp. 259-265, 2019.

[3] Y. Peng *et al.*, "Fe-ZSM-5 supported palladium nanoparticles as an efficient catalyst for toluene abatement," *Catalysis Today,* vol. 332, pp. 195-200, 2019.

[4] D. T. Sarve, S. K. Singh, and J. D. Ekhe, "Ethanol dehydration to diethyl ether over ZSM-5 and β-Zeolite supported NiW catalyst," *Inorganic Chemistry Communications,* vol. 139, p. 109397, 2022/05/01/ 2022, doi: https://doi.org/10.1016/j.inoche.2022.109397.

[5] N. Subramanian, J. Vijaya, S. Sivasanker, R. Chinnadurai, S. Thangaraju Murugan, and L. Kennedy, "Hierarchical ZSM-5 catalytic performance evaluated in the selective oxidation of styrene to benzaldehyde using TBHP," *Journal of Porous Materials,* vol. 23, 06/01 2016, doi: 10.1007/s10934-016-0129-8.

[6] I. M. S. Anekwe, B. Oboirien, and Y. M. Isa, "Catalytic conversion of bioethanol over cobalt and nickel-doped HZSM-5 zeolite catalysts," *Biofuels, Bioproducts and Biorefining,* 2023.

[7] V. P. S. Caldeira, A. G. D. Santos, S. B. C. Pergher, M. J. F. Costa, and A. S. Araujo, "USE OF A LOW-COST TEMPLATE-FREE ZSM-5 FOR ATMOSPHERIC PETROLEUM RESIDUE PYROLYSIS," *Química Nova,* vol. 39, 2016.

[8] H. Feng, C. Li, and H. Shan, "In-situ synthesis and catalytic activity of ZSM-5 zeolite," *Applied Clay Science,* vol. 42, no. 3, pp. 439-445, 2009/01/01/ 2009, doi: https://doi.org/10.1016/j.clay.2008.05.004.

[9] J. Niu, P. Rasmussen, R. Magee, and G. Nilsson, "Spatial and temporal variability of incidental nanoparticles in indoor workplaces: Impact on the characterization of point source exposures," *Environmental science. Processes & impacts,* vol. 17, 11/20 2014, doi: 10.1039/c4em00478g.

[10] B. Li, X. Lin, Y. Luo, X. Yuan, and X. Wang, "Design of active and stable bimodal nickel catalysts for methane reforming with CO2," *Fuel Processing Technology,* vol. 176, pp. 153-166, 2018.

[11] M. Shilina *et al.*, "Highly Effective Pt-Co/ZSM-5 Catalysts with Low Pt Loading for Preferential CO Oxidation in H2-Rich Mixture," *Hydrogen,* vol. 4, no. 1, pp. 154-173, 2023.

[12] M. I. Shilina, T. N. Rostovshchikova, S. A. Nikolaev, and O. V. Udalova, "Polynuclear Co-oxo cations in the catalytic oxidation of CO on Co-modified ZSM-5 zeolites," *Materials Chemistry and Physics,* vol. 223, pp. 287-298, 2019/02/01/ 2019, doi: https://doi.org/10.1016/j.matchemphys.2018.11.005.

[13] A. A. Bryzhin *et al.*, "Bimetallic Nanostructured Catalysts Prepared by Laser Electrodispersion: Structure and Activity in Redox Reactions," *ChemCatChem,* vol. 12, no. 17, pp. 4396-4405, 2020, doi: https://doi.org/10.1002/cctc.202000501.

[14] T. Rostovshchikova *et al.*, "Laser Electrodispersion of Metals for the Synthesis of Nanostructured Catalysts: Achievements and Prospects," *Russian Journal of Physical Chemistry A,* vol. 95, pp. 451-474, 2021.

[15] M. Saeidi and M. Hamidzadeh, "Co-doping a metal (Cr, Mn, Fe, Co, Ni, Cu, and Zn) on Mn/ZSM-5 catalyst and its effect on the catalytic reduction of nitrogen oxides with ammonia," *Research on Chemical Intermediates,* vol. 43, pp. 2143-2157, 2017.

[16] F. Bin, C. Song, G. Lv, J. Song, S. Wu, and X. Li, "Selective catalytic reduction of nitric oxide with ammonia over zirconium-doped copper/ZSM-5 catalysts," *Applied Catalysis B: Environmental,* vol. 150, pp. 532-543, 2014.

[17] Z. M. El-Bahy, M. M. Mohamed, F. I. Zidan, and M. S. Thabet, "Photo-degradation of acid green dye over Co–ZSM-5 catalysts prepared by incipient wetness impregnation technique," *Journal of Hazardous Materials,* vol. 153, no. 1-2, pp. 364-371, 2008.

[18] A. Jawad and S. Ahmed, "Analysis and process evaluation of metal dopant (Zr, Cr)-promoted Ga-modified ZSM-5 for the oxidative dehydrogenation of propane in the presence and absence of CO 2," *RSC advances,* vol. 13, no. 16, pp. 11081-11095, 2023.

[19] A. Jawad, F. Rezaei, and A. A. Rownaghi, "Highly efficient Pt/Mo-Fe/Ni-based Al2O3-CeO2 catalysts for dry reforming of methane," *Catalysis Today,* vol. 350, pp. 80-90, 2020/06/15/ 2020, doi: https://doi.org/10.1016/j.cattod.2019.06.004.

[20] B. Saini, A. P. Tathod, J. Diwakar, S. Arumugam, and N. Viswanadham, "Nickel nano-particles confined in ZSM-5 framework as an efficient catalyst for selective hydrodeoxygenation of lignin-derived monomers," *Biomass and Bioenergy,* vol. 157, p. 106350, 2022/02/01/ 2022, doi: https://doi.org/10.1016/j.biombioe.2022.106350.

[21] R. C. Deka, "Acidity in zeolites and their characterization by different spectroscopic methods," 1998.

[22] A. De Lucas, J. Valverde, F. Dorado, A. Romero, and I. Asencio, "Influence of the ion exchanged metal (Cu, Co, Ni and Mn) on the selective catalytic reduction of NOx over mordenite and ZSM-5," *Journal of Molecular Catalysis A: Chemical,* vol. 225, no. 1, pp. 47-58, 2005.

[23] E. F. Iliopoulou, S. Stefanidis, K. Kalogiannis, A. Delimitis, A. Lappas, and K. Triantafyllidis, "Catalytic upgrading of biomass pyrolysis vapors using transition metal-modified ZSM-5 zeolite," *Applied Catalysis B: Environmental,* vol. 127, pp. 281-290, 2012.

[24] X. Li, F. Rezaei, and A. A. Rownaghi, "Methanol-to-olefin conversion on 3D-printed ZSM-5 monolith catalysts: Effects of metal doping, mesoporosity and acid strength," *Microporous and*

Mesoporous Materials, vol. 276, pp. 1-12, 2019/03/01/ 2019, doi: https://doi.org/10.1016/j.micromeso.2018.09.016.

[25] Z. Wei *et al.*, "Steamed Zn/ZSM-5 catalysts for improved methanol aromatization with high stability," *Fuel Processing Technology,* vol. 162, pp. 66-77, 2017.

[26] V. Abdelsayed, M. W. Smith, and D. Shekhawat, "Investigation of the stability of Zn-based HZSM-5 catalysts for methane dehydroaromatization," *Applied Catalysis A: General,* Article vol. 505, pp. 365-374, 2015, doi: 10.1016/j.apcata.2015.08.017.